




ORIGINAL ARTICLE

Non-contrast preoperative MRI for determining renal perfusion and visualizing renal arteries in potential living kidney donors at 1.5 Tesla

Julian Andersson¹, Rosalie Meik¹, Mariya S. Pravdivtseva ²,
Patrick Langguth ¹, Hannes Gottschalk¹, Sam Sedaghat^{1,3},
Michael Jüptner⁴, Ioannis Koktzoglou^{5,6}, Robert R. Edelman^{5,7}, Bernd Kühn⁸,
Thorsten Feldkamp⁹, Olav Jansen¹, Marcus Both¹ and
Mona Salehi Ravesh ¹

¹Department of Radiology and Neuroradiology, University Hospital Schleswig-Holstein, Campus Kiel, Germany, ²Department of Radiology and Neuroradiology, Section Biomedical Imaging, Molecular Imaging North Competence Center (MOIN CC), University Medical Center Schleswig-Holstein (UKSH), University of Kiel, Kiel, Germany, ³Department of Diagnostic and Interventional Radiology, University Hospital Heidelberg, Heidelberg, Germany, ⁴Department of Nuclear Medicine, Molecular Imaging, Diagnostics and Therapy, University Hospital of Schleswig-Holstein, Campus Kiel, Germany, ⁵Department of Radiology, NorthShore University HealthSystem, Evanston, IL, USA, ⁶University of Chicago Pritzker School of Medicine, Chicago, IL, USA, ⁷Northwestern University Feinberg School of Medicine, Chicago, IL, USA, ⁸Siemens Healthineers AG, Erlangen, Germany and ⁹Department of Nephrology and Hypertension, University Hospital Schleswig-Holstein, Christian-Albrechts-University, Kiel, Germany

Correspondence to: Julian Andersson; E-mail: Julian.Andersson@uksh.de

ABSTRACT

Background. The aim of this work was to create and evaluate a preoperative non-contrast-enhanced (CE) magnetic resonance imaging (MRI)/angiography (MRA) protocol to assess renal function and visualize renal arteries and any abnormalities in potential living kidney donors.

Methods. In total, 28 subjects were examined using scintigraphy to determine renal function. In addition, 3D-pseudocontinuous arterial spin labeling (pCASL), a 2D-non-CE electrocardiogram-triggered radial quiescent interval slice-selective (QISS-MRA), and 4D-CE time-resolved angiography with interleaved stochastic trajectories (CE-MRA) were performed to assess renal perfusion, visualize renal arteries and detect any abnormalities. Two glomerular filtration rates [described by Gates (GFR_G) and according to the Chronic Kidney Disease Epidemiology Collaboration formula ($GFR_{CKD-EPI}$)]. The renal volumes were determined using both MRA techniques.

Results. The mean value of regional renal blood flow (rRBF) on the right side was significantly higher than that on the left. The agreements between QISS-MRA and CE-MRA concerning the assessment of absence or presence of an aberrant artery and renal arterial stenosis were perfect. The mean renal volumes measured in the right kidney with QISS-MRA

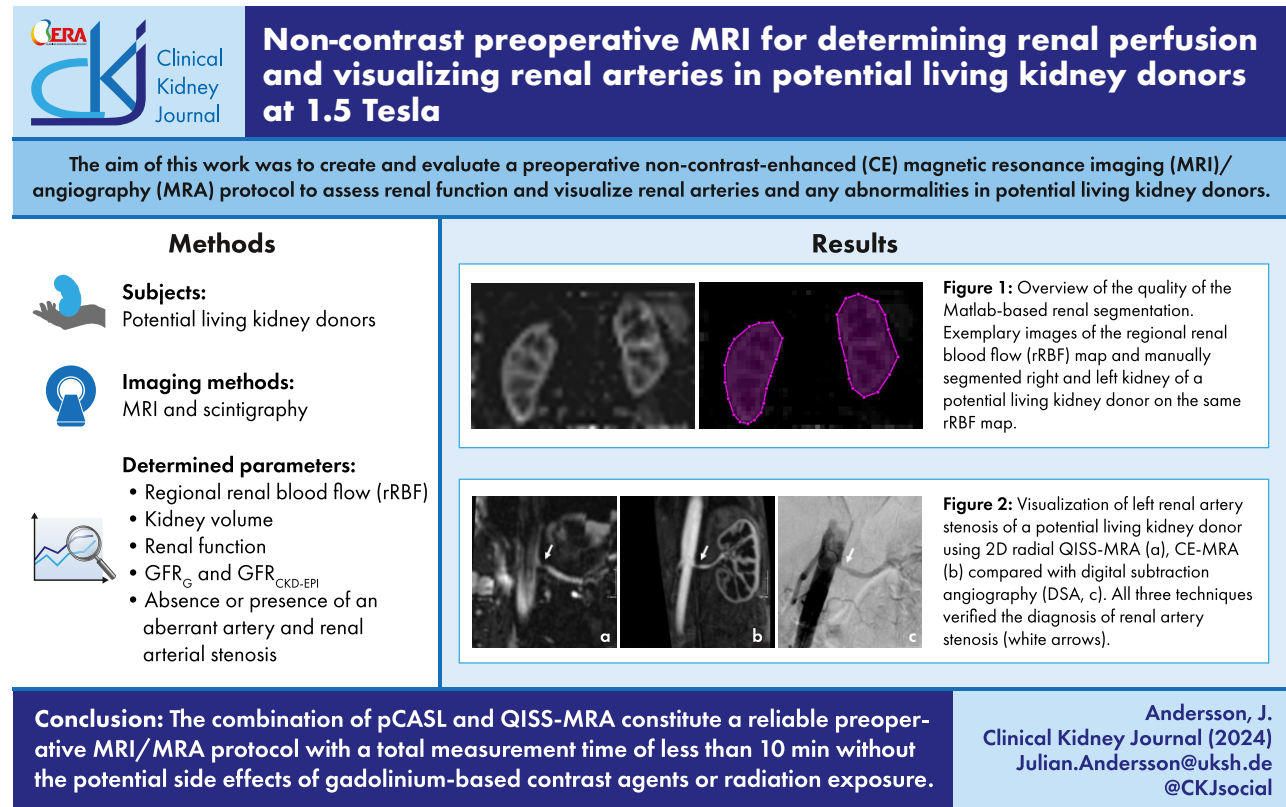
Received: 12.2.2024; Editorial decision: 15.3.2024

© The Author(s) 2024. Published by Oxford University Press on behalf of the ERA. This is an Open Access article distributed under the terms of the Creative Commons Attribution-NonCommercial License (<https://creativecommons.org/licenses/by-nc/4.0/>), which permits non-commercial re-use, distribution, and reproduction in any medium, provided the original work is properly cited. For commercial re-use, please contact journals.permissions@oup.com

were lower than the corresponding values of CE-MRA. In contrast, the mean renal volumes measured in the left kidney with both MRA techniques were similar. The correlation between the GFR_G and rRBF was compared in the same manner as that between $GFR_{CKD-EPI}$ and rRBF.

Conclusion. The combination of pCASL and QISS-MRA constitute a reliable preoperative protocol with a total measurement time of <10 min without the potential side effects of gadolinium-based contrast agents or radiation exposure.

GRAPHICAL ABSTRACT



Keywords: 2D non-contrast-enhanced (CE) electrocardiogram (ECG) radial quiescent-interval slice-selective (QISS), 3D-pseudocontinuous arterial spin labeling (pCASL), 4D-contrast-enhanced time-resolved angiography with interleaved stochastic trajectories (TWIST), ^{99m}Tc -labeled diethylenetriaminepentaacetic acid (DTPA) scintigraphy, living kidney donors

KEY LEARNING POINTS

What was known:

- To date, a standard non-CE MRI/MRA protocol to determine renal perfusion and visualize renal morphology and arterial supply has not been established or successfully implemented in clinical practice.

This study adds:

- Prior to renal transplantation, 2D radial QISS-MRA and pCASL techniques constitute a reliable non-CE MRI/MRA protocol for visualizing possible abnormalities in the renal arterial supply and assessing both renal volume and side-related renal perfusion quantitatively.

Potential impact:

- Potential clinical benefits of these techniques include use as an initial screening protocol, the possibility for repeated examinations, avoidance of possible side effects of administering gadolinium-based contrast agents and radiation exposure, and reduced peri-examination monitoring of patients compared with CE-MRA and ^{99m}Tc -labeled DTPA scintigraphy.

INTRODUCTION

The persistent shortage of kidneys for transplantation post-mortem [1] has necessitated a higher number of living kidney donors. Prior to renal transplantation, both kidneys of a potential donor must be examined to assess the current biological functional status and to clarify whether any vascular abnormalities are present that may have an impact on surgery. On one hand, the risk of transplanting a kidney with limited function or stenotic arteries can be avoided for a recipient by having this information. On the other hand, the risk of renal insufficiency due to a remaining malfunctioning kidney after transplantation and therefore a significant reduction in quality of life must be avoided for potential living kidney donors.

Currently, technetium (^{99m}Tc)-labeled diethylene-triamine-pentaacetate (DTPA) scintigraphy is used to assess renal function and contrast-enhanced (CE) magnetic resonance angiography (MRA) to visualize the renal arteries and detect any abnormalities prior to kidney transplantation [2–4].

Living kidney donors are healthy, altruistically motivated people who donate one of their kidneys to a family member. When feasible, it is therefore desirable to perform the preoperative examinations in these individuals without radiation exposure and gadolinium-based imaging techniques in order to maximize patient safety and avoid unknown long-term consequences [5, 6].

Arterial spin labeling with its variants represents a non-CE magnetic resonance imaging (MRI) technique using blood as an endogenous tracer to assess regional and global tissue perfusion in various body regions such as brain, lung, liver and kidneys [7, 8]. 2D radial electrocardiogram (ECG)-triggered quiescent-interval slice-selective (QISS) is a non-CE MRA technique that can be used to visualize the arteries in the thoracic and abdominal regions. This method has shown promising results in visualizing pulmonary artery embolism and endovascular aortic prosthesis and associated endoleaks [9, 10].

The aim of this work was to create and evaluate a non-CE preoperative MRI/MRA protocol with a total measurement time of <10 min for assessing renal function and visualizing renal arteries and any abnormalities in potential living kidney donors.

MATERIALS AND METHODS

Study patients

From 2018 to 2021, a total of 39 potential living kidney donors were consecutively referred to our university medical center for a renal MRI examination. All subjects were examined at the Clinic for Nephrology and Hypertension concerning their clinical suitability for renal transplantation. In addition, they underwent ^{99m}Tc -DTPA scintigraphy, which is a standard clinical method of examination. We excluded 11 of these 39 patients due to incomplete datasets.

Informed consent statement

This prospective single-center study (No. D 576/18 and No. D622/21) was approved by the local ethics committee of Christian-Albrechts University of Kiel. Written informed consent was obtained from the patients to publish this paper.

MRI examination

The imaging protocol consists of three techniques: (i) a research multi-inflow time pseudocontinuous arterial spin labeling

Table 1: Pertinent demographics and relevant clinical characteristics of study subjects.

Potential living kidney donors (n = 28)	
Demographic data	
Female patients (n, %)	15 (53)
Age (years)	57.1 ± 10.6
Height (cm)	174 (163; 179)
Weight (kg)	76.6 ± 14.4
Body mass index (kg/m ²)	25.3 (23.8; 27.3)
Clinical data, n (%)	
Kidney disease	0 (0.0)
Arterial hypertension	13 (46.4)
Diabetes mellitus	2 (7.1)
Hyperlipidemia	13 (46.4)
Smoking	11 (39.3)
Malignant disease	1 (3.6)

All normally distributed continuous variables are given as mean values ± standard deviations and all non-normally distributed continuous variables as median, first and third quartile values.

(pCASL) technique with single-shot 3D turbo gradient spin echo (TGSE) imaging module and background suppression was conducted in all subjects to quantitatively evaluate renal perfusion [11]. Regional renal blood flow (rRBF) maps were created automatically after performing the ASL MRI. (ii) A 2D non-CE ECG-triggered radial QISS-MRA technique was performed, which was followed by (iii) 4D-CE time-resolved angiography with interleaved stochastic trajectories (CE-MRA) for confirming or ruling out renal arterial abnormalities. All protocol parameters are listed in [Supplementary data, Table S1](#).

Demographic and clinical data

Pertinent demographics (age, weight, body mass index at examination and gender) and clinical characteristics of the study population are presented in [Table 1](#).

Image analysis

Segmentation of kidneys

The ASL datasets were processed using software developed in-house (Version 2020a; The MathWorks, Natick, MA, USA). The following steps ([Fig. 1](#)) were performed for renal segmentation: (i) the whole kidney, rRBF maps of each patient for both the right and left side ([Fig. 1a](#)), was manually segmented as a region of interest (ROI) by each reader with a closed polygonal chain ([Fig. 1b](#)). This step was repeated for each slice of the rRBF map. (ii) A binary mask was created based on each drawn ROI. All voxels inside the ROI were included in the mask. (iii) Pixel-wise perfusion values within the mask were extracted and side-separated from corresponding ROIs on each perfusion map slice for each patient. The pixel-wise perfusion values ([Fig. 1c](#) and [d](#)) from each perfusion map analyzed were exported for each renal side as a text file. The corresponding perfusion data of each renal side in a patient was summarized as one dataset. Thus, two perfusion datasets per patient were obtained, one for the right and one for the left kidney. In total, 56 perfusion datasets were analyzed statistically.

The segmentations were performed by three readers independently during separate sessions. Readers included a medical student without any experience in interpreting MRI data (reader R1, R.M.), an MR physicist with 16 years of experience in

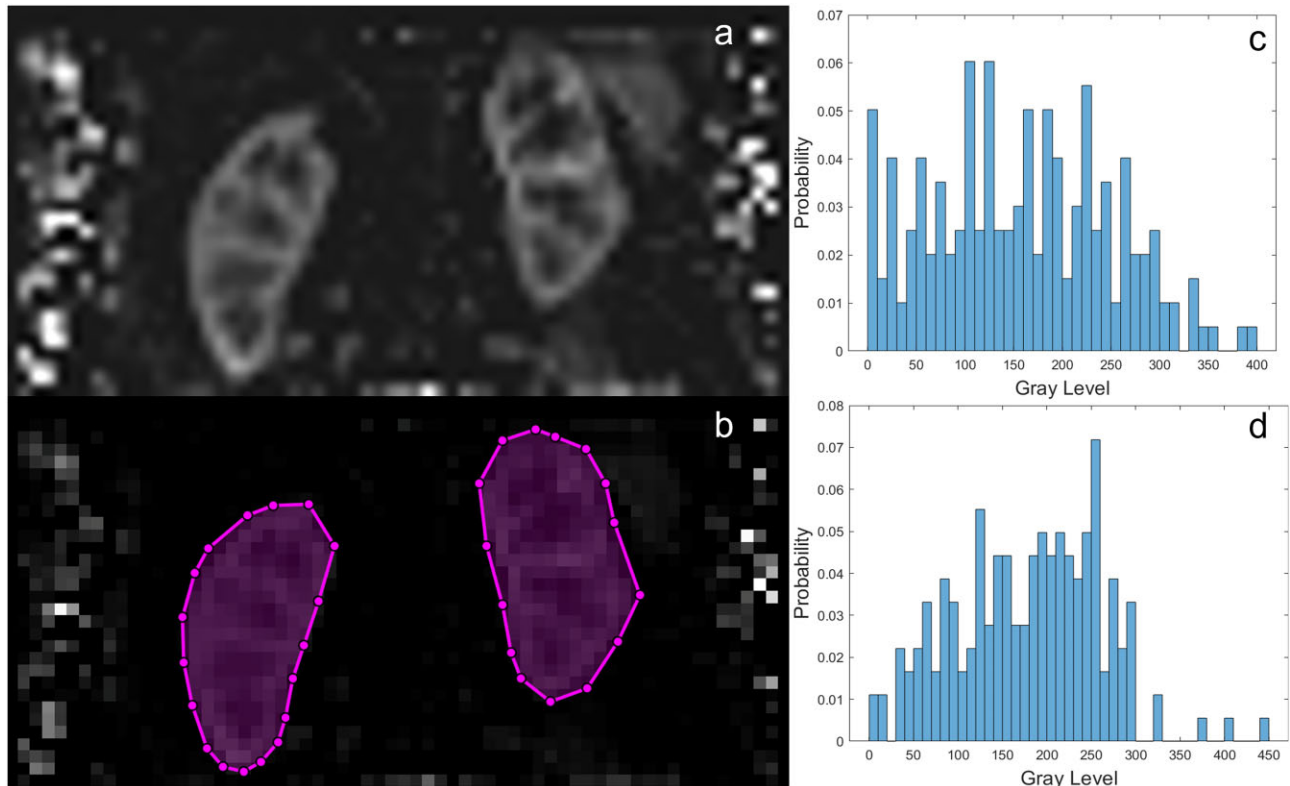


Figure 1: Overview of the quality of the Matlab-based renal segmentation. Exemplary images of the rRBF map (a) manually segmented right and left kidney of a potential living kidney donor on the same rRBF map (b), and the corresponding histograms of the rRBF distribution in the left (c) and right (d) kidney.

analyzing MR images (reader R2, M.S.R.) and a board-certified radiologist with 8 years of experience interpreting MR images (reader R3, P.L.).

Confirming or ruling out renal arterial abnormalities

Both MRA datasets of each patient were evaluated independently during separate sessions by two board-certified radiologists (J.A. and H.G.) with 7 years of experience interpreting MRA images. Image analysis was performed on a workstation (IMPAX EE, Agfa HealthCare, Bonn, Germany). The time interval between CE-MRA evaluation and QISS-MRA analysis was at least 4 weeks for each radiologist.

These two radiologists analyzed three relevant aspects of transplantation of the renal arterial blood supply: (i) absence or presence of an aberrant renal artery; (ii) absence or presence of more than one renal hilar or accessory artery; and (iii) absence or presence of a renal arterial stenosis

In addition, the presence or absence of venous contamination in images obtained with both MRA techniques was assessed. In the case of renal artery stenosis, arterial patency was not graded. To determine diagnostic performance of the MRA methods, the renal arterial abnormality results of the two radiologists per renal side were considered together as one group (28 patients \times 2 renal sides \times 2 radiologists \times 2 MRA techniques = 224 datasets per clinical angiographic questions).

Determination of renal volumes

The renal volumes were determined to investigate the impact of renal volume on the glomerular filtration rate (GFR) or on

the association between renal volume and perfusion. The length and width of each kidney were measured based on a multi-planar reconstruction of QISS-MRA and CE-MRA datasets performed on a workstation. The volume of each kidney was calculated according to an ellipsoidal formula:

$$\text{Kidney volume} = \text{width} \times \text{length} \times \text{depth} \times \frac{\pi}{6} \text{ in mL}$$

^{99m}Tc-labeled DTPA scintigraphy

The GFR was measured using the scintigraphic split method described by Gates (GFR_G) [12]. Two series of data were created for the assessment: the first one by a single board-certified specialist in nuclear medicine with an expertise of 7 years in the field of nuclear medicine, the second one by different experienced technicians under supervision of a board-certified specialist in the field of nuclear medicine directly after the examination using the Syngo.Via software (Siemens healthcare, Erlangen, Germany). Only the assessment by the aforementioned single board-certified specialist was taken for comparison with the MRI techniques. ROIs were drawn around the kidneys and in the background area in the dorsal projections [13].

Laboratory values

In all patients, GFR_{CKD-EPI} [14] in mL/min/1.73 m²; and clearance in [mL/min] as renal-relevant blood values were recorded before the MRI examination.

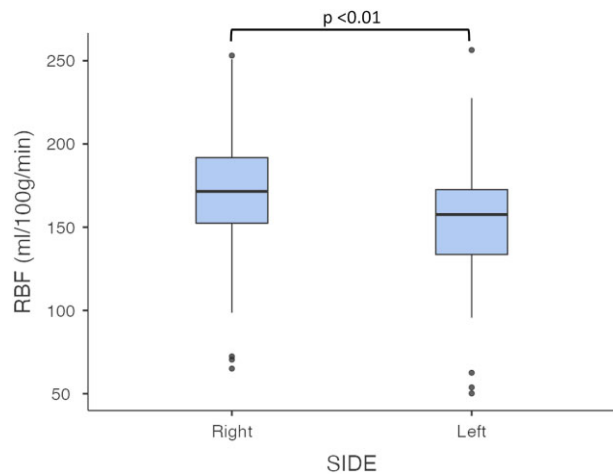


Figure 2: Comparison of rRBF in the right and left kidney. The results of all three readers were considered as one group for each side.

Statistical analysis

All statistical analyses as well as the data visualization were performed with a corresponding module of the dedicated statistical software Jamovi. Normality was tested for all variables using the Shapiro–Wilk test. Depending on the distribution of the variable, mean values and standard deviations or median values and their interquartile range were reported as summary statistics for all variables, and the P-values for comparison of two groups were obtained from a Student's t-test or a Wilcoxon signed-rank test. A P-value $< .05$ was considered statistically significant.

The two clinical methods for determining GFR were correlated using the Spearman's correlation test. The strength of the Spearman's correlation was defined as perfect ($\rho = 1.0$), very strong ($1.0 > \rho \geq 0.80$), moderate ($0.80 > \rho \geq 0.60$), fair ($0.60 > \rho \geq 0.30$) or poor ($\rho < 0.30$). CE-MRA was used as a clinical reference method for determining the diagnostic performance of the radial QISS-MRA technique for confirming and ruling out renal arterial abnormalities. Sensitivity and specificity were determined by the statistical software Jamovi.

Interobserver agreement on perfusion was assessed by quadratic, weighted concordance, stating the 95% confidence interval. Agreement was interpreted as follows: < 0.00 , poor agreement; 0.00 – 0.20 , slight agreement; 0.21 – 0.40 , fair agreement; 0.41 – 0.60 , moderate agreement; 0.61 – 0.80 , substantial agreement; or 0.81 – 1.00 , almost perfect agreement.

As a further measure of interobserver agreement, side preference was determined in terms of a binary decision in favor of the right or left side. The Fleiss' kappa (κ -value) was used to compare the three readers with each other and to compare the three readers with the scintigraphically determined side preference. The agreement was interpreted as follows: 0 , poor agreement; 0.0 – 0.20 , slight agreement; 0.21 – 0.40 , fair agreement; 0.41 – 0.60 , moderate agreement; 0.61 – 0.80 , substantial agreement; or 0.81 – 1.00 , almost perfect agreement.

RESULTS

Characteristics of study population

Relevant data for the study population are summarized in Table 1. None of the 28 subjects had known kidney disease at the time of the examination. In one patient a suspicious lesion was discovered in the MRI examination which later proved to be a pulmonary adenocarcinoma. There was no other history of malignant disease. After completing all examinations, 19 of the 28 patients were able to successfully donate one kidney. In 13 cases, the right kidney was transplanted, in 6 cases the left.

Determination of regional renal perfusion

The mean value of rRBF on the right side, considering all subjects and measurements, was higher than that on the left side (172.0 vs 158.0 mL/100 g/min, $P < .01$; Fig. 2). The mean rRBF values of the right kidney were 171.0 ± 37.4 mL/100 g/min by reader R1, 170.0 ± 39.5 mL/100 g/min by reader R2 and 169.0 ± 39.8 mL/100 g/min by reader R3 (Fig. 3a). The mean rRBF values for the left kidney (Fig. 3b) were 157.0 mL/100 g/min for all readers, with standard deviations of ± 37.1 , ± 39.0 and ± 40.3 , respectively. There were no statistically significant differences between the three readers. Therefore, the results of all three readers were further considered as one group for each side.

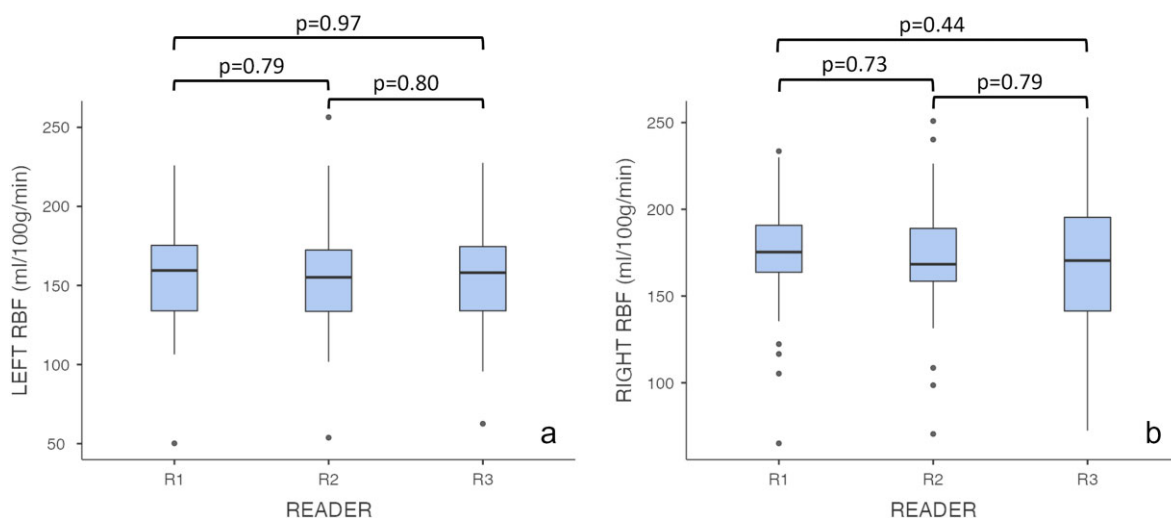


Figure 3: Interobserver agreement among three observers with different levels of experience in analyzing and segmenting perfusion MRI datasets. Panels (a) and (b) demonstrate the high interobserver agreement among all observers in the right and left kidney.

Table 2: Interobserver agreement for the determination of rRBF based on manual segmentation of kidneys by different readers.

Reader	Concordance coefficients
#1	0.921 (0.870, 0.953)
#2	0.815 (0.640, 0.909)
#3	0.859 (0.719, 0.932)

Data are given as agreement, and 95% confidence intervals are in parentheses.

Table 3: Comparison between three readers concerning preference of right kidney for transplantation based on rPBF determined using pCASL.

Reader	Side-related rRBF \pm standard deviation (%)
#1	52.2 \pm 2.7
#2	52.2 \pm 2.5
#3	51.9 \pm 2.8

Interobserver agreement concerning the determination of rRBF

Analysis of the results of three readers with different experience levels showed high reproducibility. Concordance correlation coefficients for the corresponding comparisons are summarized in Table 2. Thus, intraobserver agreement for determining global rRBF in subjects using the renal pCASL method was almost perfect.

For renal side-related percentage of perfusion distribution, an assessment of 52.2% was made for the right side (reader R1 and R2), respectively, and 51.9% in the analysis of reader R3. The standard deviations of these percentages were below 3% (Table 3). Interobserver agreement converted to side preference in terms of a binary right or left decision showed an agreement of 86% ($\kappa = 0.611$, $P < .001$), equivalent to a moderate correlation.

Determination of renal volumes

The use of QISS-MRA and CE-MRA to determine volumes of the right or the left kidneys were considered each as one group (Fig. 4). The mean right-side renal volumes measured with QISS-MRA were lower than the corresponding values of CE-MRA (134.0 ± 32.7 vs 141.0 ± 34.7 mL, $P = .002$). In contrast, the mean renal volumes on the left measured with the two MRA techniques were similar (142.0 ± 31.8 vs 146.0 ± 34.2 mL, $P = .180$).

Confirming or ruling out renal arterial abnormalities

(i) Absence or presence of an aberrant artery

The presence of an aberrant artery was detected in CE-MRA and confirmed with the QISS-MRA dataset by both radiologists in two patients. The interobserver agreement between the two angiographic methods was perfect ($\kappa = 1.0$).

(ii) Absence or presence of more than one renal artery

In six cases, both radiologists detected two supplying hilar or accessory arteries of one kidney in CE-MRA. Five of them were confirmed using QISS-MRA. The same aortic origin of one accessory hilar artery was not observed by either reader in QISS-MRA images. Thus, QISS-MRA had a sensitivity of

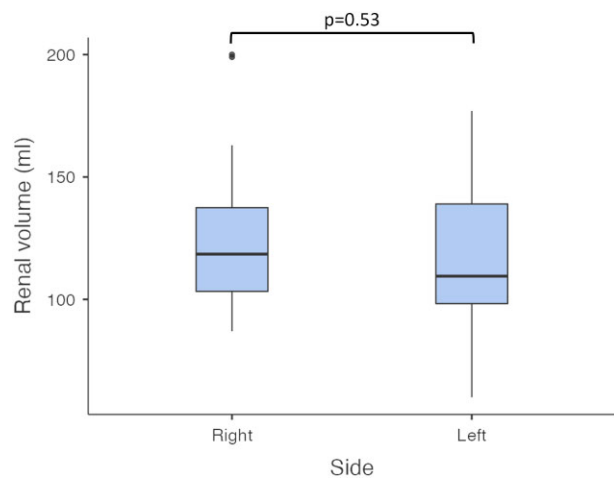


Figure 4: Comparison of volumes determined for the right and left kidney. The volumes of the right or the left kidney using QISS-MRA and CE-MRA were considered each as one group.

85.7% and a specificity of 100.0%. The interobserver agreement between the two angiographic methods was perfect ($\kappa = 1.0$).

(iii) Absence or presence of renal arterial stenosis

Both radiologists detected renal arterial stenosis (graded mild to moderate) in three arteries of two patients using both angiographic techniques (Fig. 5). The interobserver agreement between the two angiographic methods was perfect ($\kappa = 1.0$). None of the images obtained with both MRA techniques revealed diagnostic quality-impairing venous contamination.

Scintigraphic results

The mean GFR_G was 80.4 ± 20.8 mL/min/1.73 m². There were no significant differences between mean relative renal function from two analysis series in the ^{99m}Tc-labeled DTPA scintigraphy (one reader vs multi-reader: right side, 50.4 ± 4.0 vs 49.6 ± 3.7 , $P = .104$; left side, 49.6 ± 3.9 vs 50.4 ± 3.6 , $P = .154$). Comparison between these two analyses concerning a binary side selection showed a moderate agreement of 82.0% ($\kappa = 0.66$, $P < .001$).

Laboratory values

The mean $GFR_{CKD-EPI}$ was 77.1 ± 16.5 mL/min/1.73 m². The mean clearance was 110.0 ± 29.7 mL/min.

There was a significant difference between mean GFR_G and mean $GFR_{CKD-EPI}$ ($P = .009$).

Correlation between two types of GFR and rRBF

There was a fair correlation between the scintigraphically based GFR_G and rRBF ($\rho = 0.41$, $P < .001$, Table 4) and a poor correlation between the $GFR_{CKD-EPI}$ and rRBF ($\rho = 0.26$, $P < .001$, Table 4).

Correlation between kidney volumes and rRBF

There was no correlation between kidney volumes determined using both MRA techniques and rRBF (QISS-MRA: $\rho = -0.1$, $P = .13$; CE-MRA: $\rho = -0.08$, $P = .32$) and a significant correlation between kidney volumes and the $GFR_{CKD-EPI}$ (QISS-MRA: $\rho = 0.17$, $P = .025$, CE-MRA: $\rho = 0.21$, $P = .007$) and the GFR_G (QISS-MRA: $\rho = 0.28$, $P < .001$; CE-MRA: $\rho = 0.20$, $P = .008$, Table 4).

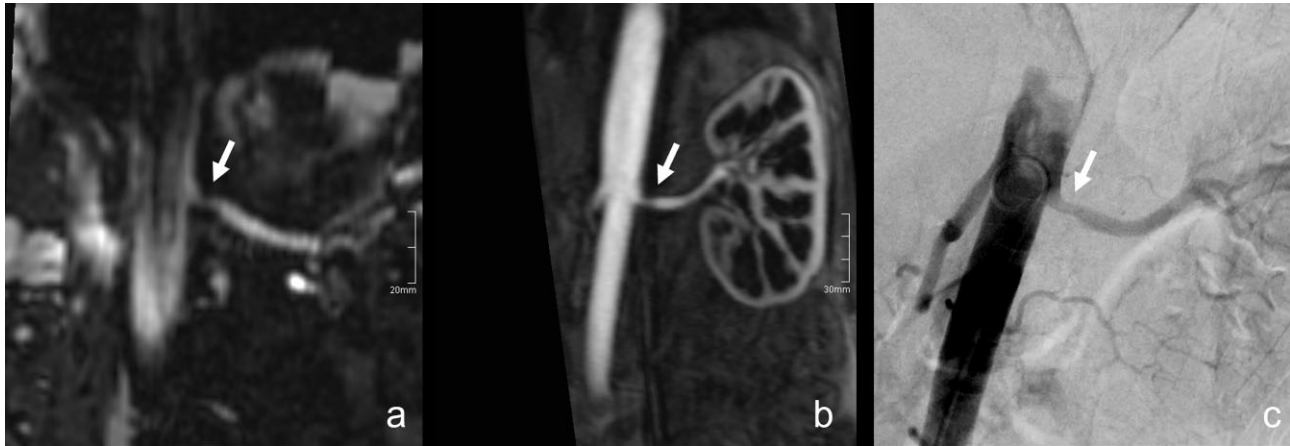


Figure 5: Visualization of left renal artery stenosis of a potential living kidney donor using 2D radial QISS-MRA (a) and CE-MRA (b) compared with digital subtraction angiography (DSA, c). All three techniques verified the diagnosis of renal artery stenosis (white arrows).

Table 4: Overview of correlation between rRBF and different demographic and clinical data of study subjects.

Correlation matrix	ρ -value	P-value
Demographic data		
Age	-0.3	<.001
Arterial hypertension	-0.176	.022
Diabetes mellitus	0.207	.007
Nicotine abuse	0.214	.005
Weight	-0.12	.534
Height	-0.06	.767
BMI	-0.21	.287
Renal volume	-0.06	.478
Clinical data		
GFR _G	0.41	<.001
GFR _{CKD-EPI}	0.26	<.001
Clearance	0.06	.483

The ρ -value indicates the Spearman's correlation coefficient, and P-values show whether the correlation coefficient is significantly different from 0.

The significant P-values are indicated in bold.

BMI, body mass index.

Correlation between renal arterial stenosis and rRBF

There was no significant correlation between the absence or presence of renal arterial stenosis and the rRBF values obtained for the right side ($\rho < 0.1$, $P = .82$) and for the left side ($\rho = 0.16$, $P = .15$, Table 4).

Correlation between side-related scintigraphic renal function and rRBF

Comparison of side preferences by scintigraphic renal function and rRBF values shows a poor agreement of 46% for the interrater reliability ($\kappa = 0.2$; $P = .003$, Table 4).

The impact of age and gender on rRBF

There was a fair, negative correlation between age and rRBF values ($\rho = -0.3$, $P < .001$). There was no significant correlation between gender and rRBF values ($\rho < 0.1$, $P = .22$, Table 4).

DISCUSSION

An MRI/MRA protocol to evaluate potential living and related kidney donors should provide essential morphological and functional information with consistent image quality and a short measurement duration. It should accurately determine the presence of significant renal volume or perfusion deficits and vascular pathology, including the presence of aberrant arteries that might alter the surgical approach.

To date, a standard non-CE MRI/MRA protocol to determine renal perfusion and visualize renal morphology and arterial supply has not been established or successfully implemented in clinical practice [7, 15–21].

In our prospective study, clinical reliability of a non-CE MRI/MRA protocol consisting of pCASL and QISS-MRA was investigated both for determining renal perfusion (function) and for diagnosing renal arterial abnormalities in potential kidney donors compared with CE-MRA and ^{99m}Tc-labeled DTPA scintigraphy, which are standard techniques for renal angiography and function.

The main findings of our study were as follows. (i) pCASL and QISS-MRA were obtained with good-to-excellent image quality in all potential kidney donors in a reasonable clinical measurement time (<10 min). (ii) The interobserver agreement between three observers for determining renal perfusion using pCASL was almost perfect. (iii) There was a significant positive correlation between GFR_G and renal perfusion and a significant negative correlation between age and renal perfusion. (iv) QISS-MRA provided high-quality images of renal arteries without limiting venous contamination- and motion-related imaging artifacts. (v) The detection of aberrant renal arteries and arterial stenosis and the determination of renal volumes with QISS-MRA was in good agreement with the results obtained using CE-MRA. (vi) There was an almost perfect correlation between QISS-MRA and CE-MRA concerning the determination of renal volumes. (vii) There was an agreement of 46% between the pCASL and ^{99m}Tc-labeled DTPA scintigraphy concerning perfusion-based side preference.

The side-separated analysis of kidney perfusion in our patients revealed that the mean value of the rRBF was slightly (8%), but significantly higher on the right side than on the left. This difference was comparable to the results from the literature in healthy subjects [22].

The high interobserver agreement among three observers with different levels of experience in analyzing and segmenting perfusion MRI datasets demonstrated that pCASL-based determination of whole kidney perfusion can be reliably used in the clinical setting.

The kidney is involved in excreting metabolic end products as well as in regulating volume status and osmolarity. Changes in renal blood flow can strongly influence these functions. Therefore, renal perfusion is a key determinant of glomerular filtration. We observed a significant correlation between renal perfusion and both GFR_G and $GFR_{CKD-EPI}$. These results are consistent with those presented in the literature [23].

Both glomerular filtration and renal blood flow are parameters for determining renal function. In the present work, these two values were examined with regard to their side-separated expression, resulting in a statistically significant agreement between ASL perfusion and side-separated scintigraphic function. The agreement between scintigraphy and ASL concerning side preference was low from a mathematical point of view. However, this does not seem to be highly relevant clinically, considering the measurement errors in both imaging techniques and the small difference in preference for one kidney side using both techniques in our healthy subjects. The individual side-separated differences are very small both scintigraphically (median side difference 5.9%) and according to the rRBF values (median side difference 4.9%). Nevertheless, it would be interesting to investigate the use of ASL to predict kidney selection in patients with unilateral renal dysfunction, as there is a well-known association of decreased rRBF values and decreased GFR in CKD patients [23–25]. In addition, ASL could be useful as a preoperative noninvasive technique to assess quantitative renal function in case of (partial) tumor nephrectomy [26].

We did not find a correlation between the renal perfusion results and the gender of our study subjects. Although our study patients were healthy living kidney donors, we observed a significant correlation between age and renal perfusion, in line with the current state of research [27, 28].

The pCASL can be performed using either a single-slice or a multi-slice technique [22, 27–30]. Multi-slice perfusion datasets provide complete coverage of kidney volume, which is convenient from a clinical point of view. Different approaches exist for manual and automatic analysis of renal perfusion maps with various software packages [22, 27–29]. In some studies, either a certain ROI was segmented on an exemplary middle slice of perfusion maps or several ROIs were drawn on different slices on the right or left kidney with differentiation between medulla and cortex or the entire kidney on the right and left side was segmented [28, 29]. In our prospective study, the entire right and left kidneys on all perfusion map slices of all patients were manually segmented using a MATLAB-based software developed in-house. We did not distinguish between medulla and cortex, in order to be able to compare these findings with those from ^{99m}Tc -labeled scintigraphy.

The volumes of the right and left kidneys could be determined using both QISS-MRA and CE-MRA. There was a significant difference between the two MRA techniques concerning the right kidney. This volume difference was about 10 mL, which would not be clinically relevant. Our volume results were in good agreement with the results from the literature using CE-MRA in healthy volunteers [31].

To the best of our knowledge, QISS-MRA was used in our study for the first time to visualize the renal arteries and determine renal volumes. The QISS-MRA proved to be a diagnostically reliable non-CE angiographic method with an accuracy of 98%–

100% compared with CE-MRA. Multiplanar reconstruction of a QISS-MRA dataset with an anisotropic voxel size produces non-diagnostic, reconstructed datasets in coronal and sagittal slice orientation due to horizontal, hyperintense imaging artifacts. To avoid this issue, it is necessary to acquire datasets in two different slice orientations (e.g. transverse and coronal or transverse and sagittal) to get information comparable to that from CE-MRA. Due to partial volume effects, an aortic outflow of an accessory renal artery was missed on datasets obtained using QISS-MRA. In addition, the result of determining renal volumes using CE-MRA and QISS-MRA only showed statistically significant differences for the right side. With relative differences in the measured volumes of <10%, this is in the range of a measurement error and is unlikely to be clinically relevant. Future studies may benefit from the use of 3D radial QISS-MRA to enable multiplanar reconstruction and increase clinical reliability and minimize the measurement error at the same time [32].

Limitations

Due to the single-center design of our study, the first limitation was the relatively small number of participants. Our study was focused on a detailed analysis of potential kidney donors without known pathological conditions in the renal tissue and the corresponding vascular system. Therefore, the second limitation was that only renally healthy subjects were included in our study.

CONCLUSION

Prior to renal transplantation, QISS-MRA and pCASL techniques constitute a reliable non-CE MRI/MRA protocol for visualizing possible abnormalities in the renal arterial supply and assessing both renal volume and side-related renal perfusion quantitatively. Potential clinical benefits of these techniques include use as an initial screening protocol, the possibility for repeated examinations, avoidance of possible side effects of administering gadolinium-based contrast agents and radiation exposure, and reduced periexamination monitoring of patients compared with CE-MRA and ^{99m}Tc -labeled DTPA scintigraphy.

SUPPLEMENTARY DATA

Supplementary data are available at [ckj](#) online.

ACKNOWLEDGEMENTS

We acknowledge financial support by Land Schleswig-Holstein within the funding programme Open Access Publikationsfonds. The authors would like to thank all patients for participating in our study. We thank our technicians for performing the MRA examinations. We warmly thank our colleagues from the Department of Nephrology and from the Department of Nuclear Medicine for their assistance in patient management.

FUNDING

Not applicable.

AUTHORS' CONTRIBUTIONS

Conceptualization, J.A. and M.S.R.; methodology, J.A. and M.S.R.; software, M.S.P., I.K., R.R.E. and B.K.; validation, not applicable; formal analysis, J.A., R.M., P.L., H.G., S.S., M.J. and M.S.R.; investigation, J.A. and M.S.R.; resources, not applicable; data

curation, J.A. and M.S.R.; writing—original draft preparation, J.A. and M.S.R.; writing—review and editing, J.A., M.S.P., I.K., R.R.E., B.K., T.F., M.B. and M.S.R.; visualization, J.A. and M.S.R.; supervision, J.A. and M.S.R.; project administration, O.J. and M.S.R.; funding acquisition, not applicable. All authors have read and agreed to the published version of the manuscript.

DATA AVAILABILITY STATEMENT

The data underlying this article will be shared on reasonable request to the corresponding author.

CONFLICT OF INTEREST STATEMENT

R.R.E. and I.K. receive research support from Siemens Healthcare. R.R.E. receives royalties from Siemens Healthcare. The other authors declare that they have no conflict of interest.

REFERENCES

1. Eurotransplant. Annual report 2022 [Internet]. 2022. Available from: <https://www.eurotransplant.org/wp-content/uploads/2023/09/Annual-Report-ET-2022.pdf>
2. Lentine KL, Kasiske BL, Levey AS et al. KDIGO Clinical Practice Guideline on the Evaluation and Care of Living Kidney Donors. *Transplantation* 2017;101:S1–109.
3. Asgari MA, Dadkhah F, Ghadian AR et al. Evaluation of the vascular anatomy in potential living kidney donors with gadolinium-enhanced magnetic resonance angiography: comparison with digital subtraction angiography and intraoperative findings. *Clin Transplant* 2011;25:481–5. <https://doi.org/10.1111/j.1399-0012.2010.01291.x>
4. Rankin SC, Jan W, Koffman CG. Noninvasive imaging of living related kidney donors: evaluation with CT angiography and gadolinium-enhanced MR angiography. *AJR Am J Roentgenol* 2001;177:349–55. <https://doi.org/10.2214/ajr.177.2.1770349>
5. Kanda T, Ishii K, Kawaguchi H et al. High signal intensity in the dentate nucleus and globus pallidus on unenhanced T1-weighted MR images: relationship with increasing cumulative dose of a gadolinium-based contrast material. *Radiology* 2014;270:834–41. <https://doi.org/10.1148/radiol.13131669>
6. Semelka RC, Ramalho M. Gadolinium deposition disease: current state of knowledge and expert opinion. *Invest Radiol* 2023;58:523–9. <https://doi.org/10.1097/RLI.0000000000000977>
7. Ku M-C, Fernández-Seara MA, Kober F et al. Noninvasive renal perfusion measurement using arterial spin labeling (ASL) MRI: basic concept. *Methods Mol Biol* 2021;2216:229–39. https://doi.org/10.1007/978-1-0716-0978-1_13
8. Hernandez-Garcia L, Aramendia-Vidaurreta V, Bolar DS et al. Recent technical developments in ASL: a review of the state of the art. *Magn Reson Med* 2022;88:2021–42. <https://doi.org/10.1002/mrm.29381>
9. Salehi Ravesh M, Tesch K, Lebenatus A et al. Clinical value of noncontrast-enhanced radial quiescent-interval slice-selective (QISS) magnetic resonance angiography for the diagnosis of acute pulmonary embolism compared to contrast-enhanced computed tomography and cartesian balanced steady-state free precession. *J Magn Reson Imaging* 2020;52:1510–24.
10. Salehi Ravesh M, Langguth P, Pfarr JA et al. Non-contrast-enhanced magnetic resonance imaging for visualization and quantification of endovascular aortic prosthesis, their endoleaks and aneurysm sacs at 1.5 T. *Magn Reson Imaging* 2019;60:164–72. <https://doi.org/10.1016/j.mri.2019.05.012>
11. Günther M, Oshio K, Feinberg DA. Single-shot 3D imaging techniques improve arterial spin labeling perfusion measurements. *Magn Reson Med* 2005;54:491–8. <https://doi.org/10.1002/mrm.20580>
12. Gates GF. Split renal function testing using Tc-99m DTPA. A rapid technique for determining differential glomerular filtration. *Clin Nucl Med* 1983;8:400–7. <https://doi.org/10.1097/00003072-198309000-00003>
13. Ma G, Shao M, Xu B et al. Glomerular filtration rate measured by 99mTc-DTPA Gates method is not significantly affected by the premature or delayed initiation of image acquisition. *Quant Imaging Med Surg* 2019;9:1103–9. <https://doi.org/10.21037/qims.2019.06.14>
14. Levey AS, Stevens LA, Schmid CH et al. A new equation to estimate glomerular filtration rate. *Ann Intern Med* 2009;150:604–12. <https://pubmed.ncbi.nlm.nih.gov/19414839/>
15. Motoyama D, Ishii Y, Takehara Y et al. Four-dimensional phase-contrast vastly undersampled isotropic projection reconstruction (4D PC-VIPR) MR evaluation of the renal arteries in transplant recipients: preliminary results. *J Magn Reson Imaging* 2017;46:595–603. <https://doi.org/10.1002/jmri.25607>
16. Serhal A, Aouad P, Serhal M et al. Evaluation of renal allograft vasculature using non-contrast 3D inversion recovery balanced steady-state free precession MRA and 2D quiescent-interval slice-selective MRA. *Explor Res Hypothesis Med* 2021;6:90–8.
17. Glockner JF, Takahashi N, Kawashima A et al. Non-contrast renal artery MRA using an inflow inversion recovery steady state free precession technique (Inhance): comparison with 3D contrast-enhanced MRA. *J Magn Reson Imaging* 2010;31:1411–8. <https://doi.org/10.1002/jmri.22194>
18. Tello R, Mitchell PJ, Witte DJ et al. Detection of renal arteries with fast spin-echo magnetic resonance imaging. *Australas Radiol* 1998;42:179–82. <https://doi.org/10.1111/j.1440-1673.1998.tb00487.x>
19. Braidy C, Daou I, Diop AD et al. Unenhanced MR angiography of renal arteries: 51 patients. *AJR Am J Roentgenol* 2012;199:W629–37. <https://doi.org/10.2214/AJR.12.8513>
20. Debatin JF, Spritzer CE, Grist TM et al. Imaging of the renal arteries: value of MR angiography. *AJR Am J Roentgenol* 1991;157:981–90. <https://doi.org/10.2214/ajr.157.5.1927823>
21. Cutajar M, Hilton R, Olsburgh J et al. Renal blood flow using arterial spin labelling MRI and calculated filtration fraction in healthy adult kidney donors pre-nephrectomy and post-nephrectomy. *Eur Radiol* 2015;25:2390–6. <https://doi.org/10.1007/s00330-015-3594-6>
22. Karger N, Biederer J, Lüsse S et al. Quantitation of renal perfusion using arterial spin labeling with FAIR-UFLARE. *Magn Reson Imaging* 2000;18:641–7. [https://doi.org/10.1016/S0730-725X\(00\)00155-7](https://doi.org/10.1016/S0730-725X(00)00155-7)
23. Gillis KA, McComb C, Patel RK et al. Non-contrast renal magnetic resonance imaging to assess perfusion and corticomedullary differentiation in health and chronic kidney disease. *Nephron* 2016;133:183–92. <https://doi.org/10.1159/000447601>

24. Zhang JL, Lee VS. Renal perfusion imaging by MRI. *J Magn Reson Imaging* 2020;52:369–79. <https://doi.org/10.1002/jmri.26911>
25. Li L-P, Tan H, Thacker JM et al. Evaluation of renal blood flow in chronic kidney disease using arterial spin labeling perfusion magnetic resonance imaging. *Kidney Int Rep* 2017;2:36–43. <https://doi.org/10.1016/j.ekir.2016.09.003>
26. Ljungberg B, Albiges L, Abu-Ghanem Y et al. European Association of Urology Guidelines on Renal Cell Carcinoma: the 2022 update. *Eur Urol* 2022;82:399–410. <https://doi.org/10.1016/j.eururo.2022.03.006>
27. Shimizu K, Kosaka N, Fujiwara Y et al. Arterial transit time-corrected renal blood flow measurement with pulsed continuous arterial spin labeling MR imaging. *Magn Reson Med Sci* 2017;16:38–44. <https://doi.org/10.2463/mrms.mp.2015-0117>
28. Cox EF, Buchanan CE, Bradley CR et al. Multiparametric renal magnetic resonance imaging: validation, interventions, and alterations in chronic kidney disease. *Front Physiol* 2017;8:696. <https://doi.org/10.3389/fphys.2017.00696>
29. Cutajar M, Thomas DL, Banks T et al. Repeatability of renal arterial spin labelling MRI in healthy subjects. *MAGMA* 2012;25:145–53. <https://doi.org/10.1007/s10334-011-0300-9>
30. Nery F, Buchanan CE, Hartevelde AA et al. Consensus-based technical recommendations for clinical translation of renal ASL MRI. *MAGMA* 2020;33:141–61. <https://doi.org/10.1007/s10334-019-00800-z>
31. van den Dool SW, Wasser MN, de Fijter JW et al. Functional renal volume: quantitative analysis at gadolinium-enhanced MR angiography—feasibility study in healthy potential kidney donors. *Radiology* 2005;236:189–95. <https://doi.org/10.1148/radiol.2361021463>
32. Edelman RR, Aherne E, Leloudas N et al. Near-isotropic non-contrast MRA of the renal and peripheral arteries using a thin-slab stack-of-stars quiescent interval slice-selective acquisition. *Magn Reson Med* 2020;83:1711–20. <https://doi.org/10.1002/mrm.28032>